UNIVERSITY OF ZIELONA GÓRA

CIVIL AND ENVIRONMENTAL ENGINEERING REPORTS

E-ISSN 2450-8594

CEER 2023; 33 (2): 0145-0157
DOI: 10.59440/ceer/174681
Original Research Article

IMPERMEABILITY EVALUATION OF CONCRETE WITH FLY ASH AGGREGATE AND PREDICTION WITH MODELLING

Gurikini LALITHA*, Chilukala Ritvik REDDY
Department of Civil Engineering, VNR Vignana Jyothi Institute of Engineering and Technology, Hyderabad Telangana, India

A b s t r a c t

Concrete is the most synthesized material in construction sector which it has aggregate as one of its components. The use of natural aggregate in concrete preparation uses a significant amount of non-renewable resources and energy, having a significant environmental impact. Multiple research projects have been conducted to safeguard natural reserves, seeking a solution to the waste disposal issue, and reduce construction costs by utilizing waste materials. FA(Fly Ash) aggregate is one such material that can be a replacement for natural aggregate. Durability parameters of concrete with Fly Ash (FA) aggregate are studied in this work as an alternative for fine aggregate. In this study, 5 concrete mixes were prepared utilizing FA aggregate in percentage substitution of 0%, 10%, 20%, 30%, and 40% for each. The quantity of cement, compaction, curing rate, concrete cover, and porosity all influence the durability of the concrete. Concrete attributes such as strength in compression, retaliation to abrasion and half-cell potential were investigated. Durability parameters of the specimens were tested after 90-day curing. The results revealed that concrete with 30% FA aggregate had the highest compressive strength, improved resistance towards abrasion and least half cell potential values. Experimentation data were used to develop comprehensive prediction models by applying support vector machine (SVM) algorithm. The SVM model analyses R2 values with an accuracy of over 97%. As a result, we can use SVM to efficiently execute prediction modelling in construction area.

Keywords: FA (Fly Ash) aggregate, Durability properties, Support-vector-machine (SVM), Prediction models, Coefficient of Determination (R^2)

1. INTRODUCTION

River sand is indeed the primary ingradient utilized as fine aggregate in the concrete manufacturing, as the most important material in the development of the high-rise structures as well as other construction projects. The mining of river sand is progressively depleting the natural resources, in which the desire for environmental preservation as well as mining bans in certain places, is exacerbating the issue of river

* Corresponding author: Lalitha Gurikini, Department of Civil Engineering, VNR Vignana Jyothi Institute of Engineering and Technology, Hyderabad Telangana, India, e-mail: godduvelagalalalitha@gmail.com

sand availability where the building sector is currently afflicted by a lack of this crucial concrete ingredient [1]. Under the present situation of scarcity of river sand and increased development in infrastructure, it is much more important to discover a concrete substitute ingradient for river sand. Fly Ash is a residue obtained in coal combustion, despite the fact that thermal power stations create significant amounts of fly ash, where limited quantity of it is currently using in concrete. Fly ash creates dumping issues and also ecological consequences by polluting the air and water on a huge scale[2]. The fly ash dust that settles by deposition and then is discharged causes pollution in the atmosphere, as well as creating dust in the summers and posing a hazard to agricultural and global health. It is apparent since approximately 56% of India's total fly ash is indeed used in numerous projects, leaving the remaining as a source of issue for sustainable solid waste management [3].Until now, the majority of studies on using fly ash in concrete has been limited to cement substitution. Considerable research was done in the earlier to produce a low-energy, cost-effective approach for generating lightweight artificial aggregate employing fly ash [4].

Aggregate make up around 70% of the concrete volume in which, fly ash derived products can be used instead of natural fine aggregate in the manufacturing of concrete could be a game-changer in terms of waste management system and preservation of natural resources [5].The fly ash aggregate production is an acceptable approach to considerably enhance the usage of fly ash, which is currently unused in most nations across the world. Experiments have recently been implemented to utilize fly ash to make lightweight aggregate using two distinct processes cold bonding and sintering. Aggregate parameters are influenced by the nature and quantity of binders used, which alters the aggregate's morphology rather than its chemical structure [6]. In this study durability parameters of concrete were examined where, the capacity to withstand abrasion, attack by chemicals, and degradation is known as durability. Concrete long-term durability is determined by its porosity where porous concrete is prone to moisture and the hazardous compounds, resulting in concrete and reinforcement degradation. The experimental programme is described thoroughly in this paper, including information of materials, test methods and apparatus. The experimental program's findings are reported, and the various measurement approaches are reviewed in terms of their possible benefits and drawbacks. A structured modeling of the strength and durability behavior of FA aggregate concrete adopting support vector machine (SVM) modeling using MATLAB algorithm was performed and presented in this manuscript.

2. MATERIALS AND METHODOLOGY

2.1. Materials

The cement is a binder agent that is employed to bind fine and coarse particles with each other. Ordinary Portland cement of grade 53, as per Indian standard IS 12269: 1987 was employed to cover the gap with the influence of water. The cement has a relative density of 3.14, an initial setting time of 35min, and standard consistency of 32%. Fine and coarse aggregate that conform to IS.383-1970 were employed [7]. Unreactive, clear, well-graded fine aggregate with angular granules were employed in preparing concrete. Natural river sand passing through a sieve of 4.75 mm and crushed angular granite aggregates of good quality with a maximum size of 20 mm were employed. Fly ash acquired from thermal power stations in Gujarat, India, and FA Aggregates were created with the sintering process. In this study, fly ash fine aggregates manufactured at a Gujarat thermal power plant were used. Fly ash aggregate is waste product, so it is relatively inexpensive compared to natural sand. This can help to reduce cost of concrete. Improved strength and increased durability: Fly ash aggregate improved the strength and durability parameters due to its chemical and mineral effects. In this research trying to check the performance of

fly ash aggregate plain concrete to test the chemical and mechanical effect of fly ash aggregate, hence no admixtures were used such that it may affect the chemical behaviour of fly ash aggregate. FA Aggregates had a relative density of 2.15. The physical parameters of materials were demonstrated in Fig 1. The properties seeking from aggregate like compatibility, adhesion strength, setting time, moisture tolerance and chemical resistance are very much resembling to natural aggregate.

2.2. In gradient Proportions

Concrete grade of M35 was employed for this study and mix design was made according to IS: 10262-1982[8]. The standard mix (M-SM) was made entirely of natural aggregate such as crushed granite and natural river sand, whereas the remaining mixes were made with an increasing percentage substitution of river sand with FA aggregates. For the entire mix proportions, a steady w/c ratio of 0.48 was employed. The percentage substitution of river sand with FA aggregates was 10%,20%, 30%, 40% [16] with that of weight of river sand, and the mix designations were given as M-FAA for FA aggregate mix and M-SM stands for standard mix. The various mix proportions were demonstrated in Table 2.

2.3. Test method

2.3.1 Compressive Strength

A compressive testing machine has been utilized to test the cast samples of size 100x100x100mm cubes and tested after curing of 7, 28 days as per IS 516[9]. The compressive force was applied consistently until specimen failed, and strength was calculated using the highest load that the specimen had sustained.

2.3.2 Underwater Abrasion Test

The abrasion test is performed using concrete specimen with a diameter of 300mm and a height of 100mm was employed, with 70 chrome steel balls of nominal size. The test procedure resembling water bodies acting on hydraulic construction. Hence under water method of testing is adopted. The test is comprised of six 12-hour intervals totaling 72 hours. The representation of test is presented in Fig.3 Percentage weight loss (PWL) and Average depth of abrasion (ADA) are considered to calculate abrasion loss. The specimen was taken from the apparatus container after every sampling interval of 12hrs, exposed specimen in the air for drying according to ASTM C1138 [10] criteria and weighed. The weight at every sampling interval was evaluated in comparison to the specimen's initial weight prior to testing to determine percentage weight loss (PWL), and the Average depth of abrasion (ADA).

2.3.3 Half cell Potential Test

This test works on the principle of forming a cell with the steel bar at the test point and the reference electrode, with the steel bar acting like anode and the reference electrode like cathode. electrode Cu/CuSO4 electrode was utilized as a reference. The rebar is linked to the voltmeter's positive, while the copper-copper sulphate electrode is linked to the voltmeter's negative. Half-cell test is performed on specimens with 100mm diameter and 200mm thick in which 12mm rebar is kept with a concrete cover of 20mm from bottom and placed in the Centre of specimen, all the samples of each mix were casted on the same day and were kept to curing for 90days.

3. SVM MODELING

3.1 Support vector machine (SVM) model

Support Vector Machine is a machine learning approach developed by Vapnik based on statistical learning theory. This hierarchical machine learning technique could be used to evaluate regressions using an SVM algorithm, which can effectively predict the findings with greater accuracy [11]. Kernel functions are employed in the SVM algorithm to restructure given data, and it then establishes a suitable range among the numerous outputs by predicting new incoming data based on these adaptations [12]. In this analysis, the Radial Basis Function (RBF) is used as the function of kernel to predict variables in MATLAB. The most prevalent forms of kernelization is the radial basis function, which is one of most widely used kernels. The RBF algorithm computes mutual resemblance, and how close they exist to one another, by considering two points X as an independent variable and Y as a dependent variable. SVM model can automatically consider the input values given through kermel function written in MATLAB.

Table 1**.** Material Parameters

Tests	**Natural Sand**	**Coarse aggregate**	**FA aggregate**
Relative Density	2.57	2.68	2.15
Water Absorption	2.2%	0.46%	6%
Loose bulk density(kg/m^3)	1542	1428	1254
Compacted Bulk density(kg/m^3)	1667	1584	1318

Table 2**.** Mix proportions for various percentage substitution of FA aggregate

Mix	% Substitution of fine aggregate	Cement (kg/m^3)	Water-cement ratio (w/c)	Water Kg/m^3	Fine aggregate Kg/m^3	FA aggregate kg/m^3	Coarse aggregate Kg/m^3
M-SM	0	410	0.48	197	634	0	1102
M-FAA10	10	410	0.48	197	570.5	63.4	1102
M-FAA20	20	410	0.48	197	507.3	126.9	1102
M-FAA30	30	410	0.48	197	443.7	190.3	1102
M-FAA40	40	410	0.48	197	380.3	253.7	1102

Table 3. Workability test readings for various mixes when sand is substituted with FA aggregate

Mix	Workability(mm)
M-SM	120
M-FAA10	115
M-FAA20	113
M-FAA30	110
M-FAA40	105

Table 4. Compressive Strength for various mixes with sand substituted with FA aggregate

Mix	7-Day (MPa)	28-day (MPa)
M-SM	25.1	37
M-FAA10	28.8	39.4
M-FAA20	30.3	42.5
M-FAA30	32.2	44.8
M-FAA40	30.8	42.1

Table 5. ADA (mm) and PWL (%) at age 90 days for different FA aggregate proportions

Time (Hours)	M-SM		M-FAA10		M-FAA20		M-FAA30		M-FAA40	
	PWL (%)	ADA (mm)	PWL (%)	ADA (mm)	PWL (%)	ADA (mm)	PWL (%)	ADA (mm)	PWL (%)	ADA (mm)
12hr	1.10	0.64	1.02	0.5	0.60	0.18	0.48	0.1	0.61	0.29
24hr	1.70	0.85	1.32	0.62	1.09	0.25	0.85	0.266	0.79	0.54
36hr	2.00	0.97	1.69	0.75	1.51	0.46	1.34	0.29	1.47	0.66
48hr	2.72	1.31	2.17	1.04	1.82	0.63	1.70	0.54	1.71	0.79
60hr	3.20	1.51	2.7	1.29	2.30	0.75	1.95	0.66	2.07	1.04
72hr	3.74	1.72	3.26	1.45	2.73	1.1	2.25	0.79	2.5	1.20

Table 6. Potential values in mV at age 90 days for different FA aggregate proportions

Mix	**Half Cell Potential(-mV)**
M-SM	−305
M-FAA10	−289
M-FAA20	−271
M-FAA30	−250
M-FAA40	−268

Table 7. Prediction values of compressive strength, Average depth of abrasion and Half-cell potential

Mix	Compressive Strength		Average Depth of Abrasion (ADA)		Half cell Potential	
	Experimental Data (MPa)	Predicted Data (MPa)	Experimental Data (mm)	Predicted Data (mm)	Experimental Data (mV)	Predicted Data (mV)
M-SM	37	37.6	1.72	1.66	-315	-297
M-FAA10	39.4	39.7	1.45	1.40	-279	-275.5
M-FAA20	42.5	42.1	1	1.04	-251	-254.4
M-FAA30	44.8	44.3	0.7	0.83	-228	-231.5
M-FAA40	42.1	41.7	1.2	1.22	-245	-248.4

Table 8**.** Results of R^2, MSE, RMSE for three datasets

Datasets	**R^2**	**MSE**	**RMSE**
Compressive strength	0.96	0.20	0.46
Average depth of abrasion	0.98	0.002	0.04
Half cell Potential	0.93	74.1	8.6

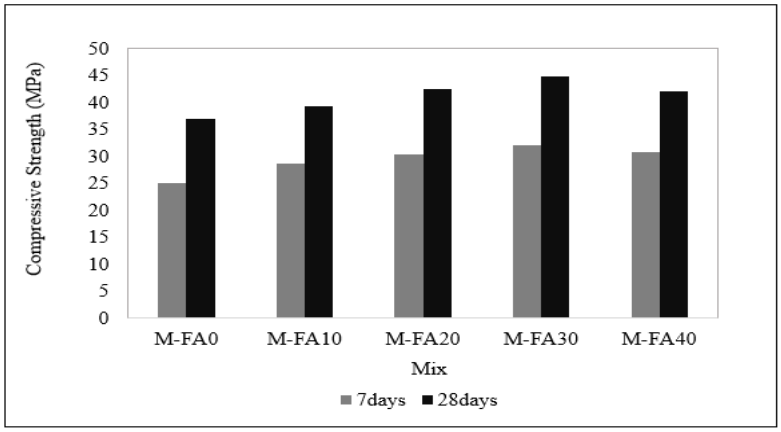

Fig. 1. Strength in compression for concrete mixes

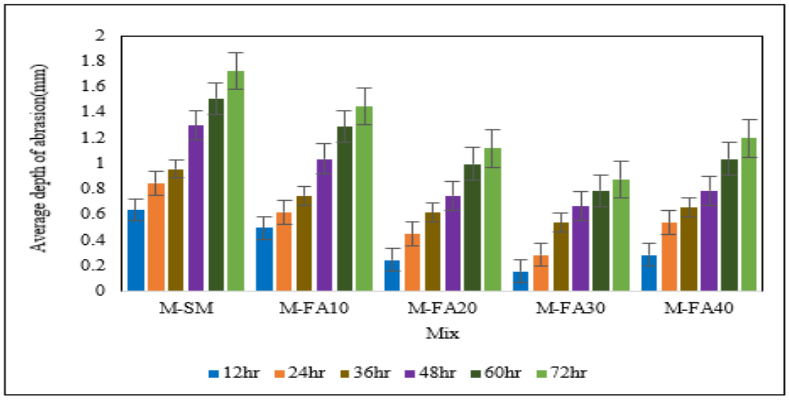

Fig.2. Bar charts for ADA (mm)

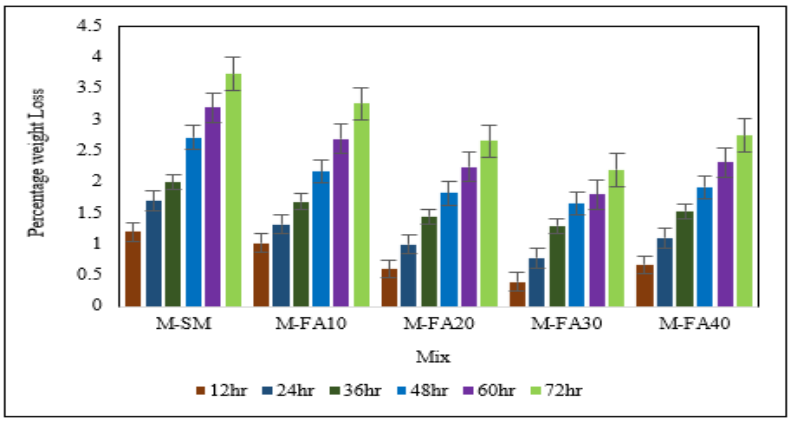

Fig. 3. BAR CHART FOR pwl (%)

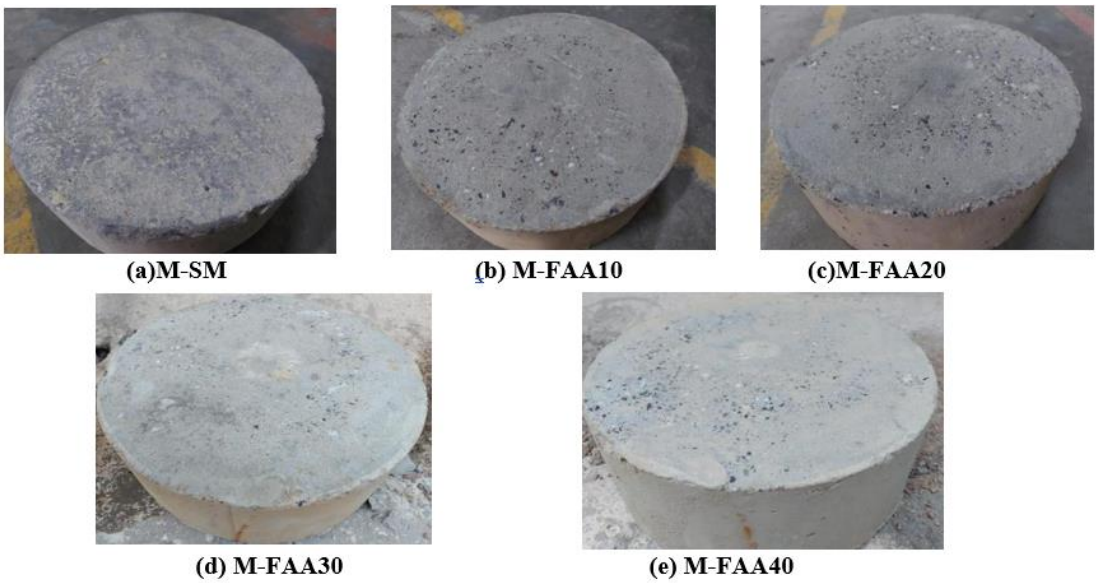

Fig. 4. Specimens following 72-hour abrasion testing

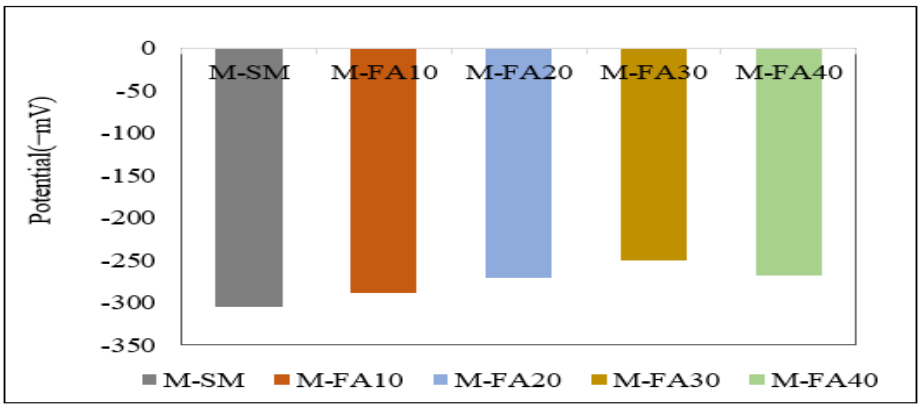

Fig. 5. Bar chart of negative Half-cell potentials (−mV) for varied FA aggregate proportions

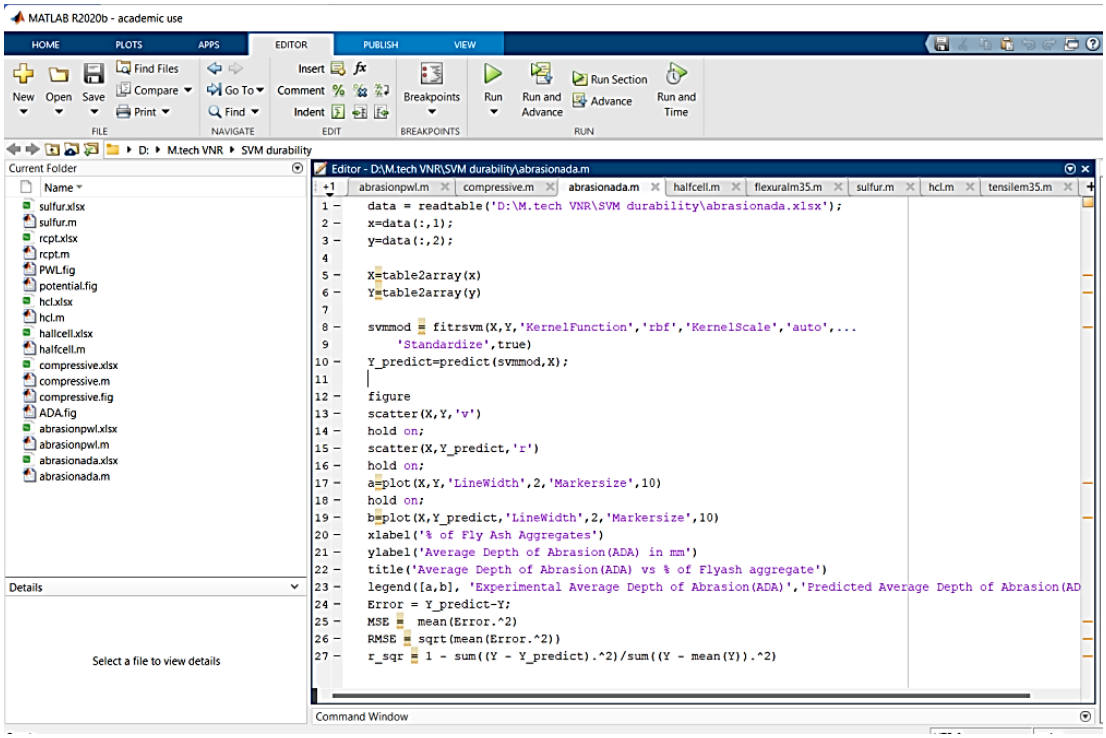

Fig.6. SVM algorithm in MATLAB

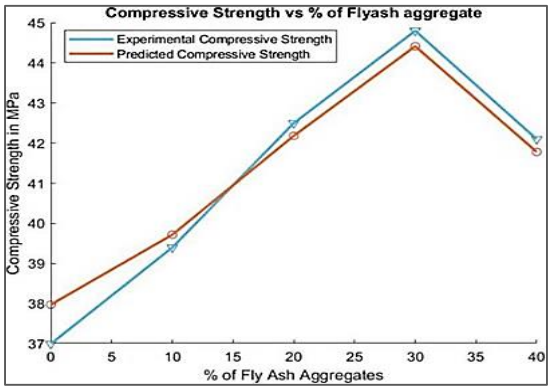

Fig.7. Model for compressive strength prediction

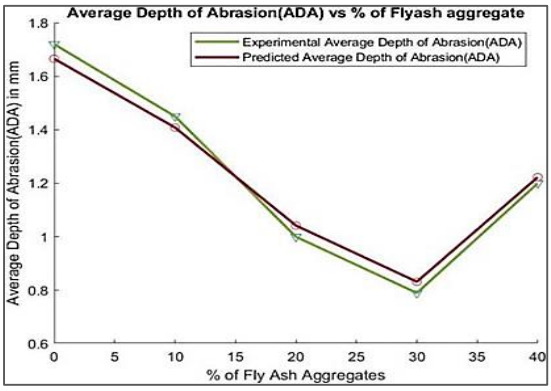

Fig.8. Model for average depth of abrasion prediction

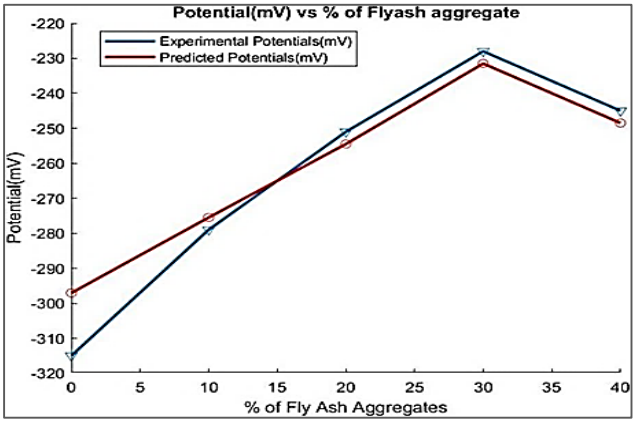

Fig.9. Model for Half-cell potential Prediction

4. RESULTS AND DISCUSSION

4.1 Workability

Table 3 shows the slump readings of fresh concrete, showing that as the percentage of sand substituted with FA aggregate increased from 0 to 40%, the concrete workability decreased significantly. FA aggregate absorbs more water than river sand during mixing which reduces the quantity of water for granular lubrication resulting in a decrease in concrete workability. The irregular surface texture of FA aggregate also resulted in increased friction of inter particles.

4.2 Compressive strength

The concrete cubes were evaluated for compression following 7 and 28 days of curing in water considering usual conditions, and the findings were demonstrated in Table 4. The strength in compression strength of M-SM specimens at 7 and 28 days were 25.1 MPa and 37 MPa, respectively. While for specimens M-FAA10, M-FAA20 and M-FAA30, the strength in compression enhanced with an increase in FA aggregate substitution. At 7 days, mixes M-FAA10, M-FAA20, M-FAA30, and M-FAA40 demonstrated a 13.1 %, 17.4 %, 22.3 %, and 18.8 % strength improvement in comparison to M-SM, which showed that concrete with FA aggregate had early strength gain. The early strength gain of concrete could be attributed to FA aggregate's higher absorption of water, which could have absorbed excess water and caused the cement paste to harden rapidly [13].At 28 days, the specimens containing 30% FA aggregate had a maximum strength value of 44.8 MPa. Up to the substitution of 30% FA aggregate in concrete, there had been a significant improvement in strength, which thereafter decreased at 40% FA aggregate. The increase in strength was attributed to rougher surface texture of FA aggregate enhanced interfacial bond among FA aggregate and cement paste with increase in FA aggregate quantity, and the pozzolanic action of FA aggregate contributes to chemical bond among FA aggregate and cement paste, resulting in high cohesion among them.The loss in strength at 40% substitution rate could be attributed due to fact that the FA aggregate was coarser than natural sand which could have reduced the fine quantity in concrete, resulting in small voids in the concrete matrix. The variation in concrete compressive strength for various mixes is depicted in Fig 1.

4.3 Underwater Abrasion Test

Results indicate that as the cumulative test time increased, Average Depth of Abrasion (ADA) and Percentage weight loss (PWL) increased. Fig.2 and Fig.3 shows the graph plotted for PWL and ADA values for all mixes obtained after testing. Following the finishing of the test, it was observed that as percentage sand substituted with FA aggregate enhanced, the ADA and PWL of concrete decreased. Table 5 shows the PWL and ADA readings of all mixes and the abraded test specimens after the completion of the 72-hour abrasion test are displayed in photographs in Fig. 4((a)–(e)). The images demonstrate that the SM specimen's surface area was significantly reduced by abrasion, due to concrete outer layer deterioration, aggregate particles were revealed, and some voids developed on the concrete specimen surfaces. The image depicts how the aggregate broke out of the matrices due to the steel balls contact and impact effects.

From Fig.2 it was seen that the mix M-SM suffered a maximum ADA of 1.72mm and the mix FA30 suffered the least abrasion of 0.88mm. Where the most amount of aggregate and cavities were exposed in M-SM specimen and FA30 specimen also had the exposure of aggregate, but no cavities were formed on the surface of specimen. The rate of abrasion of all specimens was higher in the initial hours, where most of the mortar was deteriorated on the top layer. However, once the topmost mortar layer was destroyed, the rate of abrasion reduced. As demonstrated in Fig. 4(d), the specimen FA30 had the least abrasion of the surface, with little visible exposure of aggregate particles on the surface specimen. This is a predictable propensity that as the concrete surface strengthens with the increase in concrete strength, which reduces the abrasion rate [14].

4.4 Half Cell Potential

According to ASTM C876 for, if the potentials are greater than −200 mV, the possibility of corrosion is less than 10%, and risk of corrosion is minimal. When the potentials fall around −350 to −200 mV, the risk of steel getting corroded is characterized as intermediate. Corrosion happens with a probability of more than 90% for potentials less than −350 mV, and the risk level is high. Finally, when the potential exceeds 500 mV the corrosion has already occurred severely on the steel reinforcement [15].

The half-cell potential readings were tabulated in Table 6. Following 90 curing days, the cylinders were tested, where at the time of testing the surface of the cylinders were kept saturated. The specimen M-SM had the maximum potential of −305mV, followed by the specimens M-FAA10, M-FAA20, M-FAA30, which had potentials of −289mV, −271mV, and −250mV, respectively, where the potential value decreased as the FA aggregate substitution increased. The decrease in potential values was due to a decrease in voids in concrete, which reduced the allowance of corrosion causing agents into the reinforcement. Fig.5 demonstrates the variation in potential values for each mix. The potential values of all the mixes ranged from −350 to −200 mV, indicating that the probability of steel reinforcement getting corroded is intermediate, where the mix M-FAA30 had the lowest potential value of −250mV when compared to the other mixes. The potential value of specimen M-FAA40 slightly increased to −268mV but not greater than M-SM.

4.5 SVM model results

Three datasets were adopted for SVM modeling which were designated as Compressive strength, Average Depth of Abrasion (ADA), and Half-cell Potential, where the experimental test readings were added into datasets. The RBF algorithm was used to develop prediction models with the SVM approach

in MATLAB as shown in Fig.6. Table 7 shows the prediction results achieved using the SVM model for the three datasets. Based on the graphs acquired in prediction modeling it was observed that the experimental values were relatively identical to the predicted results. Evaluating coefficient (R^2), mean squared error (MSE) and root mean squared errors (RMSE) were used to assess how well the outcomes could be predicted. The result was based on the experimental values conducted till 40% replacement only and can further extend the work to assess the model till 100% replacement.

The variables are entered into the SVM as X and Y, where X is the independent variable (% of Fly ash aggregate) and Y is the dependent variable (Compressive strength, ADA, and Half-cell Potential). The SVM algorithm is entered into MATLAB, where the command "fitrsvm" is used to carry out the prediction analysis and generate the graphs shown in Figs. 7, 8, and 9. From Fig.7, 8 and 9 it was observed that the experimental values were greater when compared to predicted models which showed that the Mixes showed good properties in strength and durability. Table 8 shows the R^2, MSE, and RMSE prediction accuracy levels for the three datasets. The R^2 values range from 0 to 1, with a higher R^2 value indicating higher accuracy. The R^2 value of three datasets were more than 0.90 which indicated that the results obtained in SVM prediction modeling was more accurate.

5. CONCLUSIONS

- The experimental results demonstrated that FA aggregate could be utilized as fine aggregate which enhances the concrete properties.
- Incorporating FA aggregate led in strength up to 44.8MPa, when compared to traditional concrete, the compressive strength has increased by 22.3 % due to the rough surface texture of FA aggregate, which promotes the cohesion among aggregate and cement paste in which by adding FA aggregate to concrete the strength properties can be improved.
- The results of the experiment revealed that the percentage weight loss (PWL) due to abrasion and average depth of abrasion (ADA) increased with an increase in test duration for all specimens. The mix M-FAA30 exhibited least PWL of 2.25% and ADA of 0.79mm.
- Half-cell potential a NDT test method was employed for determining the probability of corrosion in concrete where the mix M-FAA30 has the least potential of−228mV. The potential values of all the mixes ranged from −350 to −200 mV, indicating that the probability of steel reinforcement becoming corroded is intermediate, while the mix M-FAA30 had the lowest potential value when compared to the other mixes.
- Concrete strength and durability slightly decreased in mix M-FAA40 when compared to M-FAA30. The use of FA aggregate in concrete could be confined to 30% due to a decline in concrete properties at 40% substitution. Hence 30% can be taken as optimum %.
- SVM is a efficient predictive modelling that helped to build a comprehensive prediction model that can predict compressive strength, Average depth of abrasion, and half cell potential with above 97% accuracy. The RBF is an efficient kernel for developing prediction models.
- Fly ash aggregate is waste product, so it is relatively inexpensive compared to natural sand. This can help to reduce cost of concrete. Improved strength and increased durability: Fly ash aggregate improved the strength and durability parameters due to its chemical and mineral effects.

Financial and Ethical disclosures: This work is not supported fully or partially by any funding, organization, or agency.

Conflict of interest: The authors declare that there is no conflict of interests regarding the publication of this paper.

REFERENCES

1. Singh, M and Siddique, R 2014. Strength properties and micro-structural properties of concrete containing coal bottom ash as partial replacement of fine aggregate. *Construction and Building Materials* **50**, 246-256.
2. Soco, E and Kalembkiewicz, J 2007. Investigations of sequential leaching behavior of Cu and Zn from coal fly ash and their mobility in environmental conditions, *Journal of Hazardous Materials*, **145**, 482–487.
3. Kisku, N, Joshi, H, Ansari, M, Panda, SK and Nayak, S 2017. Dutta, S.C., A critical review and assessment for usage of recycled aggregate as sustainable construction material, *Construction Building Materials*, 131, 721–740.
4. Samuel, MF, Brooke Nicholas, GJ, Leonard, G M and Ingham, J M, 2011. Mixture design development and performance verification of structural lightweight pumice aggregate concrete. *Journal of Materials in Civil Engineering* **23(8),** 1211–9.
5. Patel, SK, Majhi, RK, Satpathy, HP and Nayak, AN 2019. Durability and microstructural properties of lightweight concrete manufactured with fly ash cenosphere and sintered fly ash aggregate. *Construction and Building Materials* **226**, 579-590.
6. Ramamurthy, K and Harikrishnan, KI 2006. Influence of binders on properties of sintered fly ash aggregate. *construction and building materials* **28(1)**, 33–8.
7. IS: 383-1970, Specifications for Coarse and Fine Aggregate from Natural Sources for Concrete, *Bureau of Indian Standards*, New Delhi, India, 1970.
8. IS 10262, Indian Standard Concrete Mix Proportioning – Guidelines, *Bureau of Indian Standards*, New Delhi, 2009.
9. IS: 516, Indian Standard Methods of Tests for Strength Concrete, *Bureau of Indian Standards*, New Delhi, 1959 [Reaffirmed in 1999].
10. ASTM C1138-97, Standard Test Method for Abrasion Resistance of Concrete (Underwater Method), *ASTM International*, West Conshohocken, USA, 1997, 1–4.
11. Dai, F, Nie, G H and Chen, Y 2020. The municipal solid waste generation distribution prediction system based on FIG–GA-SVR model. *Journal of Material Cycles and Waste Management* **22(5),** 1352-1369.
12. Muller, KR, Mika, S, Ratsch, G, Tsuda, K and Scholkopf, B 2001. An introduction to kernel-based learning algorithms. *IEEE transactions on neural networks* **12(2)**, 181-201.
13. Patel, SK, Majhi, RK, Satpathy, HP, and Nayak, AN 2019. Durability and microstructural properties of lightweight concrete manufactured with fly ash cenosphere and sintered fly ash aggregate. *Construction and Building Materials* **226**, 579-590.
14. Abid, SR, Hilo, AN, Ayoob, NS and Daek, YH 2019. Underwater abrasion of steel fiber-reinforced self-compacting concrete. *Case Studies in Construction Materials* **11**, 1-17.
15. Adriman, R, Ibrahim, IBM, Huzni, S, Fonna, S and Ariffin, AK 2022. Improving half-cell potential survey through computational inverse analysis for quantitative corrosion profiling. *Case Studies in Construction Materials*, **16,** p.e00854.
16. Lalitha, G, Sashidhar, C and Ramachandrudu, C 2020. Evaluation of Mechanical Properties on M30 Concrete Crushed Waste Glass as Fine Aggregate. *Journal of Green Engineering* **10(9)**, 5242-5249